Congestion-Distortion Optimized Video Transmission Over Ad Hoc Networks

Xiaoqing Zhu, Eric Setton and Bernd Girod

Information Systems Laboratory, Department of Electrical Engineering
Stanford University, Stanford, CA94305-9510, USA
{*zhuxq, esetton, bgirod*}*@stanford.edu*

Abstract

The performance of low-latency video streaming with multipath routing over ad hoc networks is studied. As the available transmission rate of individual links in an ad hoc network is typically limited due to power and bandwidth constraints, a single node transmitting multimedia data may impact the overall network congestion and may therefore need to limit its rate while striving for the highest sustainable video quality. For this purpose, optimal routing algorithms which seek to minimize congestion by optimally distributing traffic over multiple paths are attractive. To predict the end-to-end rate-distortion tradeoff, we develop a model which captures both the impact of encoder quantization and of packet loss due to network congestion on the overall video quality. The validity of the model is confirmed by network simulations performed with different routing algorithms, latency requirements and encoding structures.

Key words: video distortion model, video streaming, ad hoc network, multipath routing

1 Introduction

In ad hoc networks, nodes self-organize to create a mesh, in which each node can act as a source, a destination or a relay for traffic. The flexibility of such networks may be leveraged in a variety of contexts where the deployment of a fixed infrastructure may be unfeasible or impractical. For example, in search-and-rescue operations, establishing connectivity between wireless terminals would allow voice and data communication in a disaster area without the presence of cellular base stations. By using an ad-hoc mesh, one can achieve both better coverage and capacity as compared to two-way radios.

There are many technical issues yet to be addressed to support real-time multimedia applications over wireless ad hoc networks. The high data rates characterizing voice and video streams, and the tight delay constraints required for real-time communication and interactivity are difficult to accommodate in a network where node mobility and multipath fading may lead to unfavorable wireless channel conditions. In addition, limited power at wireless nodes and interference between neighboring transmitters result in a bandwidth-limited environment with relatively low capacity on each link.

Prior work on distortion models for packetized video streaming has analyzed the impact of packet loss on video quality when a media stream is sent over an error-prone channel. In [1], the performance of a generic video encoder is modeled, as well as the effect of packet loss for a time-invariant channel. In [2], the effect of specific loss patterns on decoded video quality is analyzed. These models focus on the case when bandwidth is not the limiting factor, and have not addressed how network congestion may affect the received video quality and how the action of a single user may affect the overall network condition. For ad hoc wireless networks, this problem cannot be overlooked. The goal of this paper, therefore, is to model the rate-distortion tradeoff of low latency video streaming over ad hoc networks, by incorporating both the impact of encoder performance and the influence of network congestion.

Decoded video quality largely depends on the sustainable rate provided by the network layer. While traditional routing algorithms have shared the goal of minimizing the number of hops between source and destination, and maintaining complete routing tables at the routers, for ad hoc networks routing needs to be revisited. Source routing algorithms, in which one or multiple routes are provided on-demand for each stream, are usually considered a better alternative to table-based routing, as network conditions are constantly changing [3,4]. In this case, new optimization criteria such as the quality of the path(s) or the available bandwidth of the route(s) may prove more useful than the number of hops [5,6]. Another routing strategy is to minimize the overall network congestion by partitioning flows optimally over multiple paths [7]. The combination of multipath routing with multiple description video coding has often been proposed to improve the error resilliency for video streaming over both the Internet and ad hoc wireless networks [9–11]. Multipath routing can also aggregate link rate for a single video stream and hence sustain higher video bit-rates while simultaneously avoiding congestion by load balancing [12–14]. In our work, the benefit of multipath routing is attained in terms of a higher supportable video rate, as the route selection and video traffic partitioning are both performed in a congestion-minimized fashion.

The rest of the paper is organized as follows. In the next section, we present a video distortion model which captures the influence of both the encoder performance and network congestion. The proposed congestion-optimized routing is compared to a simpler load balancing approach in Section 3. Experimental results for two video sequences over a simulated ad hoc wireless network are presented in Section 4, where we discuss the impact of using different routing

algorithms, coding structures and latency requirements on the reconstructed video quality.

2 Video Distortion Model

In live streaming applications, compressed video is transmitted over a network at a given rate. It is desirable to achieve end-to-end delays of no more than a few hundred milliseconds. When a packet does not arrive at the receiver by its playout deadline, to avoid interruptions, the decoder conceals the missing information and the playout continues at the cost of higher distortion. Decoded video quality at the receiver is therefore affected by two factors: quantization errors introduced at the encoder while compressing the media stream, and packet loss either caused by transmission errors or due to late arrivals. These two contributions have different characteristics. Typically, the distortion introduced by quantization is evenly distributed across the encoded frames and is determined by the encoding bit-rate. This contrasts with the impact of packet loss which usually introduces decoding errors (i.e. higher distortion) in the frame containing the missing packet(s). Because of the predictive nature of the compressed video stream, this error will propagate to subsequent frames. Usually, these errors tend to decay over time due to intra-macroblock insertions and in-loop filtering (see e.g. [15]). Error propagation is eventually stopped when an intra-coded frame is received.
Using *Mean Square Error (MSE)* as the criterion, a video distortion model can be derived based on [1]. The decoded video distortion, denoted by D_{dec}, comprises two terms:

$$D_{dec} = D_{enc} + D_{loss}, \tag{1}$$

where the distortion introduced by quantization at the encoder is denoted by D_{enc}, and the additional distortion caused by packet loss is denoted by D_{loss}. The expressions for both factors are described in the following sections.

2.1 Encoder Distortion Model

The distortion introduced by encoder quantization is a decreasing convex function of the encoding rate. In [1], this rate-distortion tradeoff is modeled by the simple formula:

$$D_{enc} = D_0 + \frac{\theta}{(R - R_0)}, \tag{2}$$

where R is the rate of the video stream, and D_0, θ and R_0 are model parameters. Using nonlinear regression techniques, these parameters can be estimated from empirical rate-distortion curves, with three or more trial encodings at different rates.
Note that the parameters D_0, θ and R_0 need to be estimated separately for each video sequence and for different encoder settings, such as frame rate, GOP length and encoding structure (e.g., with or without B frames). As an illustration, Fig. 1 shows the fit for two QCIF sequences, *Foreman* and *Mother and Daughter*, encoded with an H.264 encoder [16].

2.2 Distortion Induced by Packet Loss

The contribution of packet losses to decoded video distortion was also analyzed in detail in [1], where this term was shown to be linearly related to the packet loss rate, denoted by P_{loss}, assuming a small loss rate. D_{loss} can be written as:

$$D_{loss} = \kappa P_{loss}. \tag{3}$$

The sensitivity of the sequence to packet loss, κ, depends on parameters related to the compressed video sequence, such as the proportion of intra-coded macroblocks and the effectiveness of error concealment at the decoder. The packet loss rate P_{loss} reflects the combined rate of random losses and late arrivals of video packets. In a bandwidth-limited ad hoc network, this combined loss rate can be further modeled based on the M/M/1 queuing model. In this case, the delay distribution of packets over a single link is exponential:

$$\mathbf{Prob}\{Delay > T\} = e^{-\lambda T}, \tag{4}$$

where λ is determined by the average delay:

$$\mathbf{E}\{Delay\} = \frac{1}{\lambda} = \frac{L}{C - R}. \tag{5}$$

In (5), C is the capacity of the link, R is the traffic rate on that link, and L is the average packet size. Note that in practice, video packets are transmitted over the network at regular intervals along one or possibly several multi-hop paths. This contrasts with our assumption of a single-link M/M/1 model, where packet arrivals follow the Poisson process and each packet goes through a single link with exponentially distributed service time. Nevertheless, in a bandwidth-limited ad hoc network, the end-to-end delay of packet delivery is dominated by the queuing delay at the bottleneck link. Hence the empirical delay distribution for realistic traffic patterns can still be modelled by

an exponential. We therefore derive the expression of packet loss ratio using the M/M/1 model, and later fit the parameters with experimental data from realistic traffic patterns:

$$\mathbf{Prob}\{Delay > T\} = e^{-(C'-R)T/L'}. \tag{6}$$

In (6), T is the playout deadline for the video stream and R is the total transmitted rate. The parameter C' is related to the maximum video rate supported by the set of paths provided by the routing algorithm. It depends on the link capacities and rate of background traffic over the selected routes. L' depends on the average packet size. These two parameters need to be determined empirically from end-to-end delay statistics over the network. They are independent of the video content streamed by the source. Figure 2 illustrates how to estimate L' and C' from experimental packet delay distributions.
Together with a random packet loss rate P_r due to transmission errors, the total packet loss rate is then:

$$P_{loss} = P_r + (1 - P_r)e^{-(C'-R)T/L'}. \tag{7}$$

The total distortion from packet loss can be expressed as:

$$D_{loss} = \kappa P_{loss} = \kappa(P_r + (1 - P_r)e^{-(C'-R)T/L'}), \tag{8}$$

where the sensitivity factor κ depends on the video sequence and the coding parameters.

2.3 Total Distortion

Combining (1)-(8), the received video distortion can be expressed as:

$$\begin{aligned} D_{dec} &= D_{enc} + D_{loss} \\ &= D_0 + \frac{\theta}{R - R_0} + \kappa(P_r + (1 - P_r)e^{-(C'-R)T/L'}). \end{aligned} \tag{9}$$

The proposed formula models the impact of the rate on the video distortion. At lower rates, reconstructed video quality is limited by coarse quantization, whereas at high rates, the video stream will cause more network congestion and therefore will lead to longer packet delays. These, in turn, translate into higher loss rates, hence reduced video quality. For live video steaming in bandwidth-limited environments, we therefore expect to achieve maximum decoded quality for some intermediate rate. In fact, the optimal transmission rate R^* can

be numerically solved from the model by setting to zero the derivative of (9) with respect to R, which reduces to:

$$\sqrt{\frac{\theta L}{\kappa T(1-P_r)}}e^{\frac{(C'-R^*)T}{2L'}} - R^* + R_0 = 0. \quad (10)$$

Figure 3 shows the rate-PSNR tradeoff when streaming the video sequence *Foreman* or *Mother and Daughter* over the simulated ad hoc network described in Section 4. The model is fit to experimental data for two cases. In the first case, the only losses considered are due to late arrivals; in the second, an additional end-to-end random loss rate of 1% is considered. The bell-shape of the curves illustrates that the highest performance is obtained when the streaming rate achieves the optimal tradeoff between compression quality and self-inflicted congestion. The theoretical optimal operating rates computed by numerically solving (10) from the models match closely with experimental readings. The difference in decoded video quality caused by the additional 1% random packet loss is more pronounced in *Foreman* than in *Mother and Daughter*. Indeed, the sensitivity to packet loss for *Foreman*, denoted by κ in (3) is higher as the sequence contains more motion and losses are therefore harder to conceal.

3 Multipath Routing

The model presented in Section 2 highlights the impact of congestion on the performance of a low-latency video streaming application. For a given set of paths, congestion limits the sustainable rate for low-latency video streaming. To support higher rates, multiple routes achieving higher aggregate bandwidth must be chosen at the network layer. This motivates the use of congestion-aware routing which seeks to make efficient use of the network resources by distributing traffic over the network. In the following, we describe and compare two such routing algorithms of varying complexity: congestion-optimized routing and load balancing.

3.1 Congestion-optimized routing

The problem of congestion-optimized routing on a generic network has been studied extensively, see, e.g. [7]. Assuming the M/M/1 queuing model, the average delay over the network has a closed-form expression which only depends on the capacity of the links and on the network traffic flows. This average delay is a convex function of the flows and can be used as a measure of con-

gestion. Minimizing the network congestion results in the following convex optimization problem:

$$Min. \quad \sum_{(i,j)} \frac{f_{ij} + F_{ij}}{C_{ij} - F_{ij} - fij}. \tag{11}$$

In (11), the sum is taken over all the links of the network. C is a constant matrix denoting the available capacity between each directional link. The matrix F indicates the rate of background traffic on each link and f is the variable matrix indicating how new traffic are assigned to each link of the network. In addition, the variables f_{ij}'s need to satisfy several linear constraints including rate constraints at the source and at the destination, flow continuity at each node and flow positivity.
Such formulations are attractive as they allow higher rates to be transmitted over the network without causing excessive delay on any of the links. They can be solved efficiently both by centralized or by distributed algorithms [17,18]. In both cases, deriving the optimal solution requires that link state information such as capacity and flow be dynamically estimated and exchanged between nodes in the network. This may not be easily implementable in a mobile wireless network where conditions may change frequently and where information exchange among the nodes creates additional interference. In addition, solutions to (11) are often too complex to be implemented and need to be simplified in practical systems. This is done, for example, by recursively extracting the largest flows from the optimal flow assignment solution. Readers are referred to [14] for greater details of the path selection process. Despite the practical limitations in complexity and scalability, congestion-optimized routing is interesting as it offers an upper-bound on the achievable performance.

3.2 Load-balancing routing

A simple alternative to congestion-optimized routing is load-balancing in which traffic flows are distributed proportionally over a given set of network paths. To avoid overwhelming a link, traffic is distributed proportionally to the bottleneck residual capacity of each path. Compared to congestion-optimized routing, less information needs to be collected at the source. However, this kind of traffic partitioning is not, in itself, a routing algorithm, as it relies on the pre-computation of a set of routes. In practice, it could be applied in conjunction with an algorithm which performs this first step, such as Dynamic Source Routing (DSR) [19] with one of its multipath extensions as proposed in [10] and [6]. When the set of paths are independent, load-balancing approaches the solution to congestion-minimized flow partitioning at high rates.

4 Simulation Results

Simulations are performed in ns-2 [20] over a network with 15 stationary nodes randomly placed in a 100m-by-100m square. As an example, Fig. 4 shows the routing and traffic partitioning results for streaming 100 kbps of video between two nodes. Link capacity (C_{ij}) from Node i to Node j are computed as a function of the *signal-to-interference-plus-noise-ratio* ($SINR_{ij}$):

$$C_{ij} = \frac{B}{2}\log(1 + \gamma SINR_{ij}), \tag{12}$$

where B is the bandwidth and the coding gain $\gamma < 1$ indicates the performance gap of a practical channel coder with respect to Shannon's information-theoretical limit. Here, the network model assumes that the underlying media access control follows a fixed CDMA procedure, where multiple nodes can simultaneously transmit and receive, and the effect of interference is captured in the calculation of the $SINR$ values. For a more realistic network such as one operating under the IEEE 802.11b protocol, the link capacities also depend on the traffic rate and contention from adjacent flows and therefore it will be a more challenging task to determine their values. The investigation of such network models is part of future research.

Video traffic is streamed from Node 1 to Node 5. For simplicity, we use the Constant Bit Rate (CBR) model to represent video traffic and assume each frame fits in one packet. Background traffic is specified as a random process with exponentially distributed packet sizes and arrival intervals. The average rate of background traffic on each link is randomly selected in the range of $0 - 50\%$ of the link capacity. The impact of using different traffic patterns for both the video and background flows is shown to be small, as in Table 1.

The QCIF video sequences *Foreman* and *Mother and Daughter* are encoded and decoded with H.264 at 30 frames per second, using various quantization levels and for different *Group of Pictures (GOP)* lengths. For most of the following experiments, no random packet loss is introduced. Packets are dropped only if they do not arrive at the receiver by the playout deadline. In this case, previous-frame concealment is used. Decoded video quality is measured in terms of *peak-signal-to-noise-ratio (PSNR)* of the luminance component. For each experiment, the video sequence is looped for more than 400 times, and the average values of all realizations are calculated, which can be interpreted as the expected performance of the algorithm in a snapshot of time for the given network.

Table 1
Comparison of average packet loss ratio and end-to-end delay for two different traffic patterns. In scenario A, the background traffic follows the CBR model whereas actual encoded packet sizes are used to represent the video traffic; in scenario B, the background traffic has exponentially distributed arrival intervals and packet sizes (with an average of 100 bytes) whereas the video traffic follows the CBR model. The simulation is performed with the *Foreman* sequence, using single-path routing and setting the playout deadline at 350ms.

Rate (kbps)	Loss ratio (%)		End-to-end delay (ms)	
	Scenario A	Scenario B	Scenario A	Scenario B
28.3	0	0	32.9	31.1
31.6	0	0	37.8	36.1
35.2	0	0	44.2	42.4
39.9	0	0	52.7	50.8
43.6	0	0	60.0	58.2
49.7	0	0	74.3	72.4
54.8	0	0	85.3	83.2
61.8	0	0	104.9	102.6
70.3	0.1	0.1	126.9	124.3
78.6	2.7	2.5	165.9	163.5
89.1	99.1	99.1	1302.1	1195.8
102.3	99.5	99.5	1765.7	1576.2
114.5	99.8	99.8	1982.7	1868.7

4.1 Influence of routing

Figure 5 shows the effect of multipath routing and traffic partitioning on network congestion, which is measured in terms of average link delay. The result for exponentially distributed traffic is plotted together with the curves from the M/M/1 model. Both the congestion-optimized scheme and load balancing are tested with various number of paths.

The benefit of multipath routing is illustrated by the fact that a higher data rate can be supported with an increased number of paths. Compared to single-path routing, the supported data rate is tripled for 3-path routing and is increased four times when using 6 paths. The performance gain of congestion-optimized traffic partitioning over load balancing is also demonstrated in the figure. When only one path is used, both schemes are equivalent. For 3-path routing, the links of the paths are largely independent. In this case, the op-

timal traffic partitioning strategy reduces to load-balancing at high rates, as illustrated in Fig. 6, which shows the traffic partitioning results for both algorithms at different rates. This is because network congestion is dominated by the backlog at the bottleneck link of each path. In the case of 6-path routing, however, due to the presence of shared links, the network cannot be accurately modeled as a set of parallel paths. Therefore, load balancing can no longer maintain a good performance, while the congestion-optimized scheme still makes use of network resources efficiently and supports a significantly higher data rate without causing excessive network congestion.
The relative performance of the different routing and traffic partitioning algorithms is reflected in Fig. 7, which plots the tradeoff of decoded video quality versus transmission rate for *Foreman*. The playout deadline is set to 500 ms. The individual points obtained from experiments are fitted with the solid lines predicted from the proposed distortion model. While the low rate region of the curve follows closely the encoder rate-PSNR performance as few packets experience excessive delays, there is a sharp degradation when the rate exceeds a certain threshold, as predicted by the model. This is the region where some bottleneck link is overwhelmed by the video stream, and received video quality is predominantly affected by late packet arrivals. By using more paths for routing and by partitioning traffic in a congestion-optimized fashion, the video stream can be transmitted at higher rates without incurring excessive network congestion, hence decoded with better quality. Compared to the single-path case, 6-path routing improves the performance by up to 6 dB in terms of PSNR. Congestion-optimized routing also outperforms load-balancing by 1 dB in PSNR.

4.2 Influence of the playout deadline

Figure 8 shows the decoded video quality as a function of transmission rate for both sequences. Video packets are streamed over 6 paths and the playout deadline is set to 350 ms or 500 ms. When the transmitted rate exceeds a certain threshold, self-inflicted congestion causes too much delay on the network to meet the delay constraint and the received video quality eventually degrades. For a lower latency tolerance, this degradation occurs for rates well below the capacity. In this case, even a slight increase in queuing delay affects the performance. In other words, effective capacity is reduced as the delay constraint becomes tighter. When the delay tolerance is lax, the drop off is sharper and occurs at rates closer to the total available transmission rate.

4.3 Influence of Coding Structure

The model can also be used to study the impact of the coding structure on the performance of video streaming. For example, Fig. 9 illustrates the rate-distortion performance when the interval between successive intra-coded frames is varied between 5 frames and 25 frames. Not surprisingly, the coding efficiency of the encoder increases for longer group of pictures (GOP). This is conveyed in Fig. 9 by the relative placement of the curves at low bit-rates, which also illustrates the diminishing returns of the gain. On the other hand, longer GOPs also cause an increase in the sensitivity to packet loss. Indeed, due to predictive coding, a decoding error will propagate until the next intra-coded frame, which leads to higher quality degradation for longer GOPs. This effect translates into a sharper performance degradation at higher rates for the curves representing longer GOPs in Fig. 9. Higher performance is achieved for longer GOP length. Note however, that this is only true when there are no random losses on the network and the only quality degradation is caused by self-inflicted congestion. When an additional 1% end-to-end loss rate is considered, the relative performance for the three coding structures changes, as illustrated in Fig. 10. In this case the stream with an intermediate GOP length of 15 performs slightly better. The performance in all cases is accurately predicted by the distortion model.

5 Conclusion and Future Work

We propose a video distortion model for live video streaming in wireless ad hoc networks. The model incorporates contributions from both encoder distortion and packet loss due to network congestion. The optimal rate for video streaming achieves the optimal tradeoff between compression quality and self-inflicted congestion. The total available rate can be increased, provided an optimized routing algorithm is used to distribute traffic wisely over the network. Experimental results for two video sequences over a simulated ad hoc wireless network are presented for different routing scenarios, packet loss rates, coding structures and playout deadlines. The model captures the influence of these different parameters and can be used to predict the end-to-end rate-distortion performance.

Further work is needed for an online estimate of the model parameters, so that the optimal video rate can be determined on-the-fly by actively probing the network conditions. Experiments with multiple sender-receiver pairs are in progress to investigate how the video streams influence each other. It is also part of future research to extend the work to other types of wireless networks, and to consider the effect of mobility for the proposed multipath routing algorithm.

6 Acknowledgments

The authors would like to thank Professors Andrea Goldsmith and Fouad Tobagi at Stanford University for many insightful discussions. This work is supported, in part, by NSF Grant CCR0325639.

References

[1] K. Stuhlmüller, N. Färber and M. Link and B. Girod, "Analysis of video transmission over lossy channels", *IEEE Journal on Selected Areas in Communications*, vol. 18, no. 6, pp. 1012-1032, June 2000.

[2] Y. J. Liang, J. G. Apostolopoulos and B. Girod, "Analysis of packet loss for compressed video: does burst length matter?", *IEEE International Conference on Acoustics, Speech and Signal Processing (ICASSP'03)*, Hong Kong, April 2003.

[3] E. M. Royer and C.-K. Toh, "A review of current routing protocols for ad hoc mobile wireless networks", *IEEE Personal Communications*, pp.46-55, April 1999.

[4] S.-J. Lee, M. Gerla and C.-K. Toh, "A Simulation Study of Table-Driven and On-Demand Routing Protocols for Mobile Ad Hoc Networks", *IEEE Network*, pp. 48-54, August 1999.

[5] D. De Couto, D. Aguayo, B. Chambers and R. Morris, "Performance of multihop wireless networks: shortest path is not enough", *Proceedings of the First Workshop on Hot Topics in Networking*, Princeton, USA, October 2002.

[6] W. Wei and A. Zakhor, "Robust multipath source routing protocol (RMPSR) for video communication over wireless ad hoc network" *Proceedings of International Conference on Multimedia and Expo(ICME'04)*, Taipei, Taiwan, July 2004.

[7] L. Kleinrock, "Queuing Systems, Volume II: Computer Applications", *Wiley Interscience*, New York, 1976.

[8] D. Bertsekas and R. Gallager, "Data Networks", *Prentice Hall, NJ*, 1987.

[9] J. G. Apostolopoulos and S. J. Wee, "Unbalanced multiple description video communication using path diversity", *IEEE International Conference on Image Processing (ICIP'01)*, Thessaloniki, Greece, October, 2001.

[10] S. Mao and S. Lin, S. S. Panar, Y. Wang and E. Celebi, "Video transport over ad hoc networks: multistream coding with multipath transport", *IEEE Journal on Selected Areas in Communications, Special Issue on Recent Advances in Wireless Multimedia*, vol. 21, no. 10, pp.1721-1737, December 2003.

[11] A. C. Begen, Y. Altunbasak, O. Ergun and M. H. Ammar, "Multi-path selection for multiple description video streaming over overlay networks", *EURASIP Signal Processing: Image Communication*, vol. 20/1, pp. 39-60, January, 2005.

[12] L. Zhang, Z. Zhao, Y. Shu, L. Wang and O. Yang, "Load balancing of multipath source routing in ad hoc networks", *Proceedings IEEE International Communications Conference (ICC'02)*, New York, U.S.A, April 2002.

[13] J. Chen and S.-H. G. Chan and V. O. K. Li, "Multipath routing for video delivery over bandwidth-limited networks", *IEEE Journal on Selected Areas in Communications*, vol. 22, no. 10, pp. 1920 - 1932, December 2004.

[14] E. Setton, X. Zhu and B. Girod, "Congestion-optimized multipath streaming of video over ad hoc wireless networks", *International Conference on Multimedia and Expo (ICME'04)'*, Taipei, Taiwan, July 2004.

[15] N. Färber, "Feedback-based error control for robust video transmission", Doctoral Dissertation. *Department of Electrical Engineering, University of Erlangen*, 2000.

[16] ITU-T and ISO/IEC JTC 1, *Advanced video coding for generic audiovisual services, ITU-T Recommendation H.264 - ISO/IEC 14496-10(AVC)*, 2003.

[17] Y. Nesterov and A. Nemirovsky, "Interior point polynomial methods in convex programming", *Studies in Applied Mathematics, SIAM*, vol. 13, Philadelphia, USA, 1994

[18] J. Tsitsiklis and D. Bertsekas, "Distributed asynchronous optimal routing in data networks", *IEEE Transactions on Automatic Control*, vol. AC-31, pp.325-332, April 1986.

[19] D. B. Johnson and D. A. Maltz, "Dynamic source routing in ad hoc wireless networks", *Mobile Computing*, Kluwer Academic Publishers, 1996.

[20] "NS-2", *http://www.isi.edu/nsnam/ns/*.

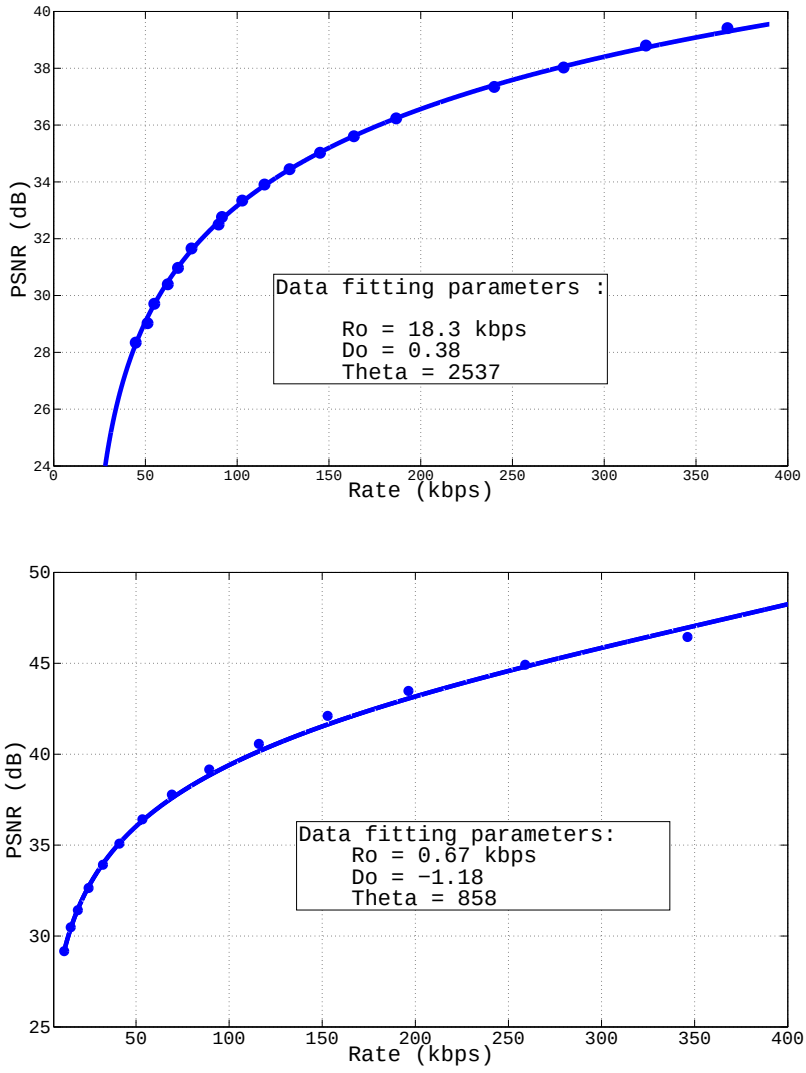

Fig. 1. Fitting the encoder distortion for the *Foreman* (top) and *Mother and Daughter* (bottom) QCIF sequences at 30 frames per second and GOP length of 15.

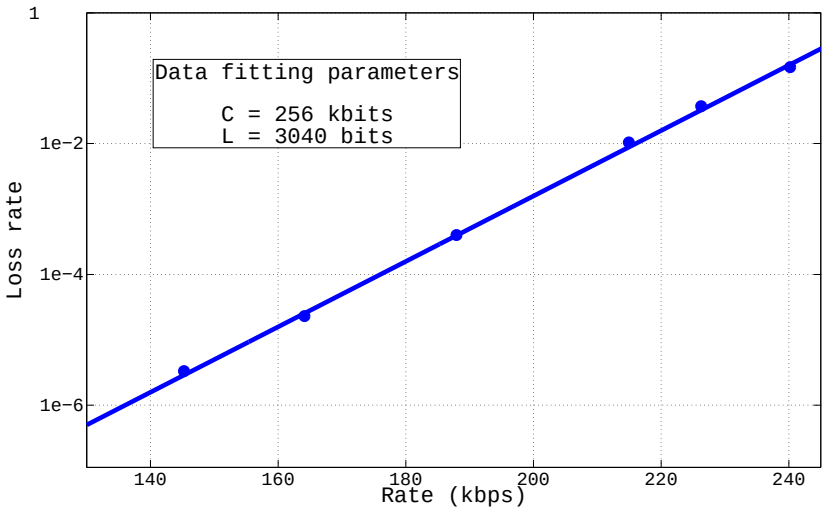

Fig. 2. The exponential fit of the loss rate is a simple linear regression of its logarithm.

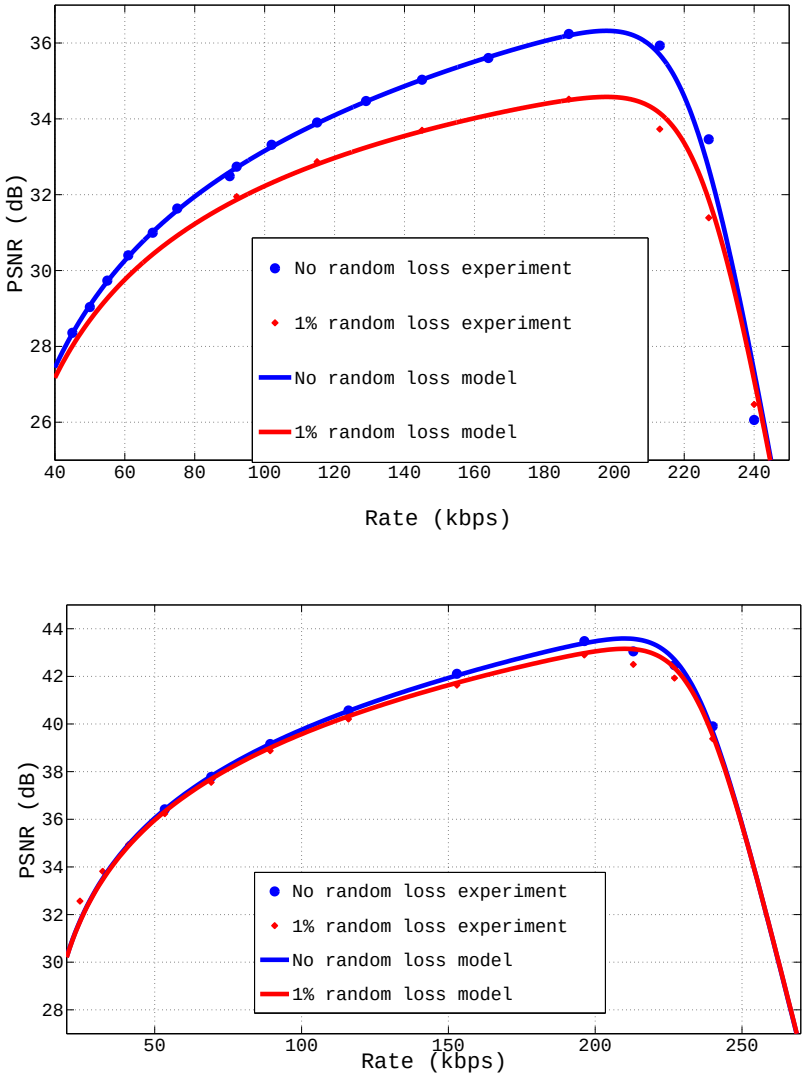

Fig. 3. Decoded video quality model and experimental data for *Foreman* (top) and *Mother and Daughter* (bottom) QCIF sequences at 30 frames per second and GOP length of 15, with 3-path routing over the network and a playout deadline of 350ms. The solid lines in show the performance without random packet loss over the network ($P_r = 0.0$); the dotted lines correspond to an additional random packet loss of 1% ($P_r = 0.01$). The value of κ is 750 for *Foreman* and 30 for *Mother and Daughter*. The optimal rates R^* as calculated from the model are 195 kbps and 210 kbps for the two sequences respectively.

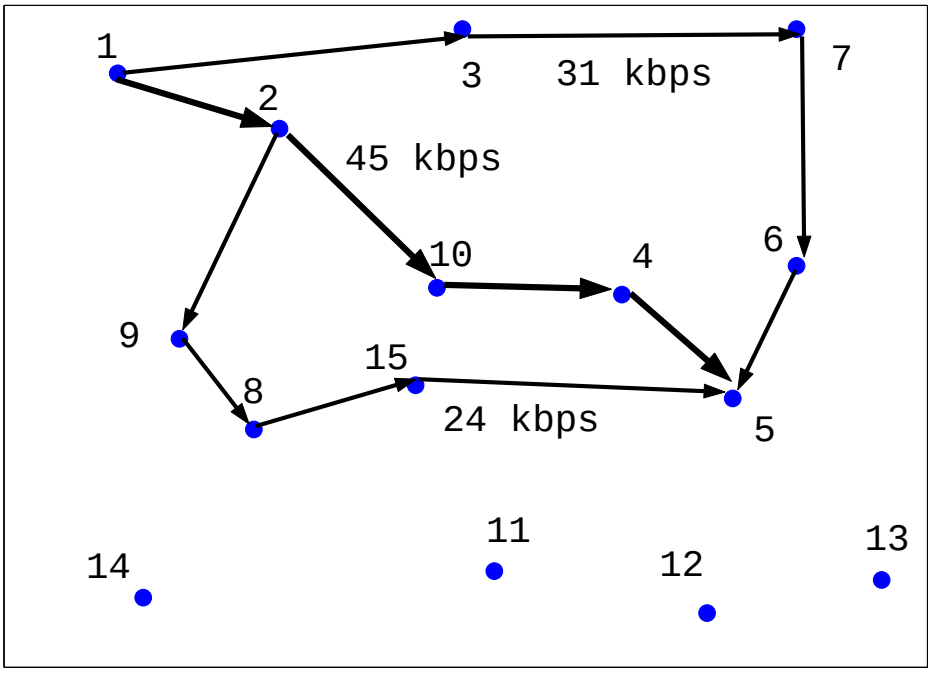

Fig. 4. Optimized routing and traffic partitioning example for streaming 100 kbps over 3 paths.

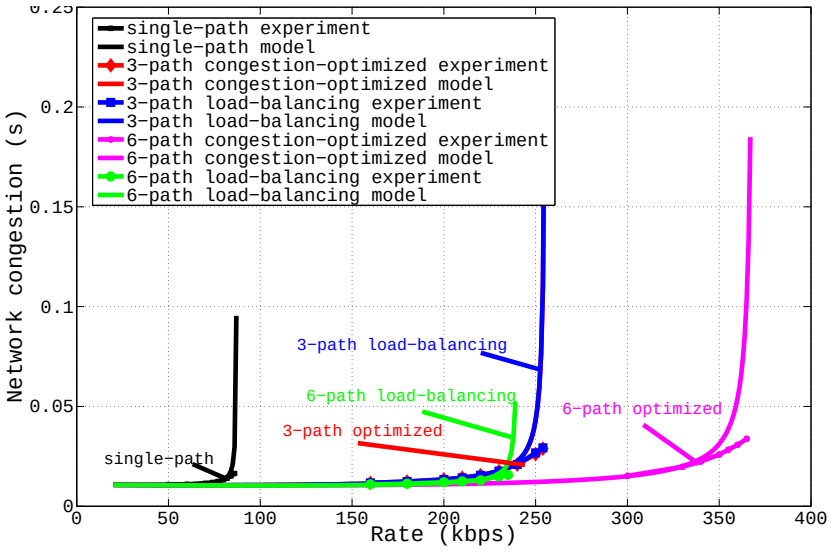

Fig. 5. Average network congestion for data transmission using routing over 1 path, 3 paths and 6 paths.

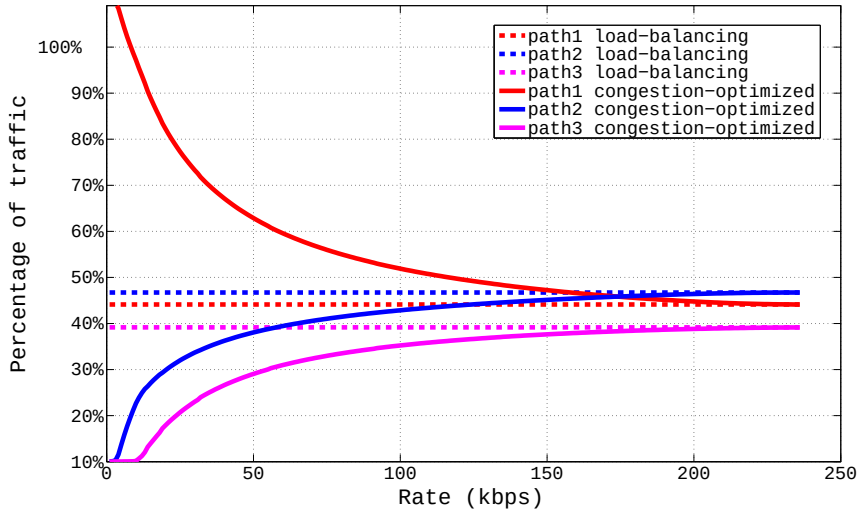

Fig. 6. Traffic partition for 3-path routing using the congestion-optimized algorithm (in solid lines) and the load balancing approach (in dashed lines). At higher rates, the congestion-optimized solution reduces to that of load balancing.

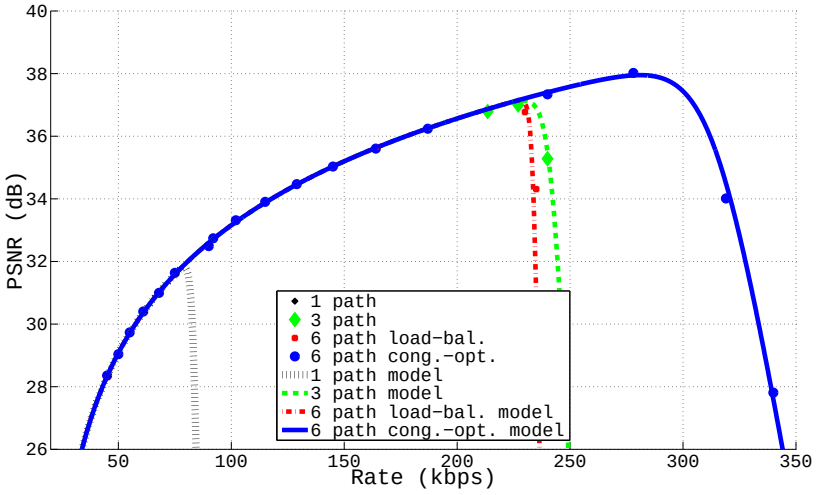

Fig. 7. Rate-PSNR performance for live video streaming using single-path, 3-path and 6-path routing with different traffic partitioning algorithms.

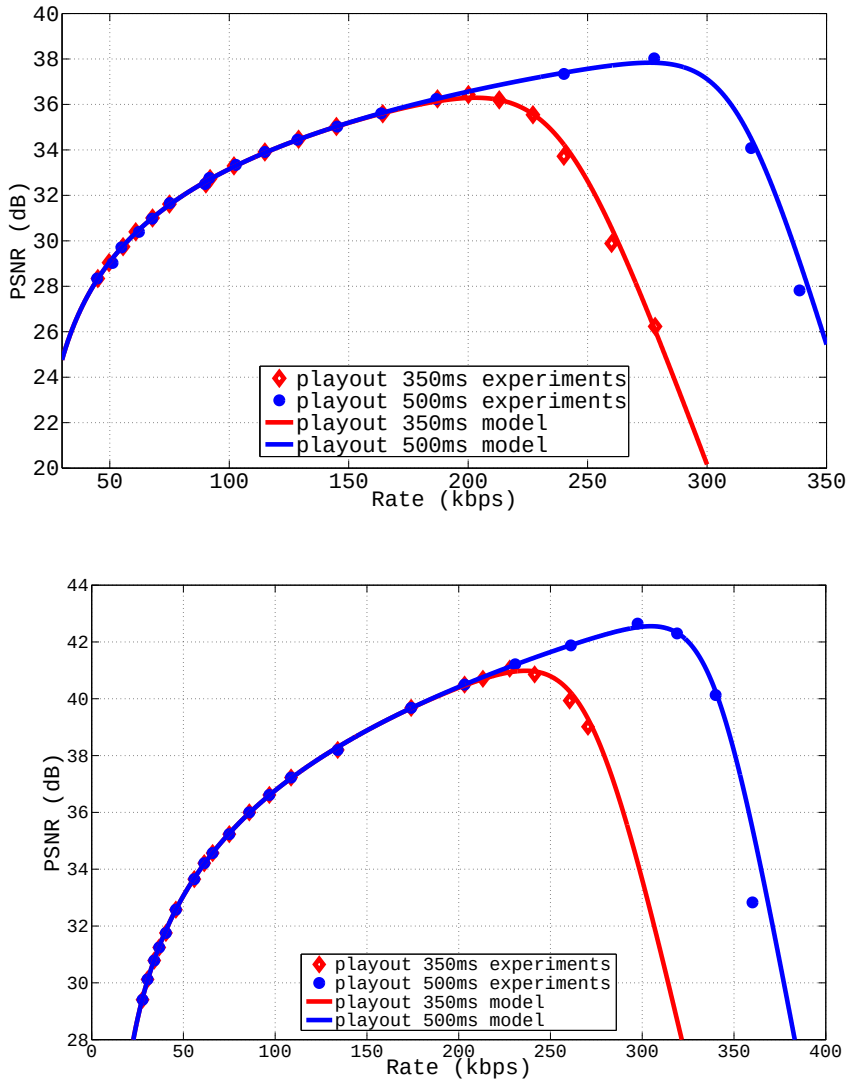

Fig. 8. Rate-PSNR performance for live video streaming of *Foreman* (top) and *Mother and Daughter* (bottom) using 6-path routing with congestion-minimized traffic partitioning.

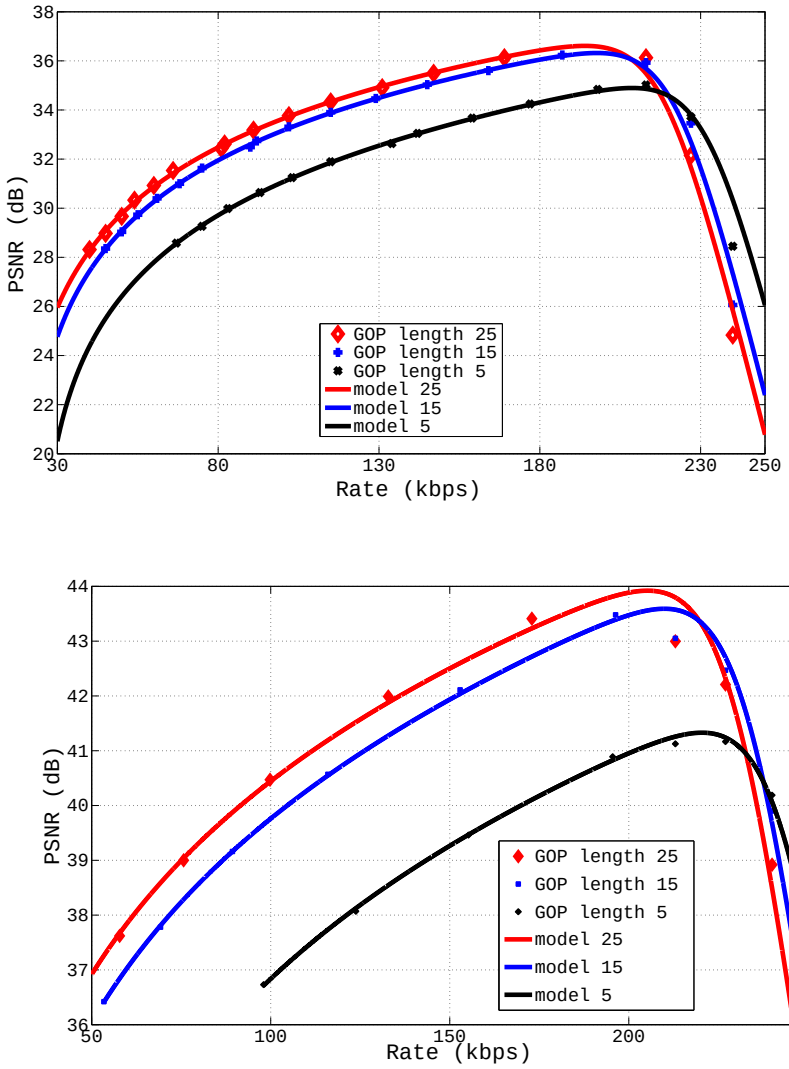

Fig. 9. Rate-PSNR performance for live video streaming of *Foreman* (top) and *Mother and Daughter* (bottom) using 3-path routing with congestion-minimized traffic partition and different GOP lengths.

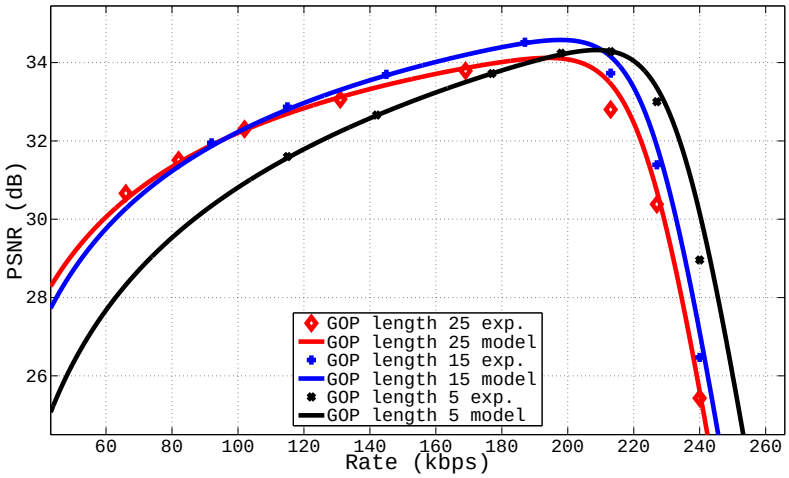

Fig. 10. Rate-PSNR performance for live video streaming of *Foreman* using 3-path routing with congestion-minimized traffic partition and different GOP lengths with an additional end-to-end packet loss rate of 1%